THE UNIVERSITY OF MICHIGAN

DEPARTMENT OF ELECTRICAL ENGINEERING
Electromagnetic Materials Laboratory

Final Report

STUDY PROGRAM FOR A MAGNETIC TIMER UTILIZING THE PROPAGATION OF DOMAIN WALLS

W. W. Raymond
D. M. Grimes

ORA Project 03775

under contract with:

DIAMOND ORDNANCE FUZE LABORATORIES
ORDNANCE CORPS, DEPARTMENT OF THE ARMY
CONTRACT DA-49-186-502-ORD-945
WASHINGTON, D. C.

administered through:

OFFICE OF RESEARCH ADMINISTRATION ANN ARBOR

June 1961

FOREWORD

The following is the final report on a study program undertaken to investigate the possible use of controlled domain wall propagation in a magnetic material as a continuously variable time delay device. This program was jointly financed through DOFL Contract DA-99-186-502-ORD-945, and AFOSR Contract 49(638)-986. This report is jointly being used as a final report to DOFL and as a technical report to AFOSR.

The equation of domain wall propagation is developed in terms of the fundamental parameters of the magnetic material. Conditions required for precisely controlled wall motion are discussed in terms of the shape and physical characteristics of the media. Those external parameters which influence propagation are elaborated on in view of how they may be controlled to optimize the shape and velocity of the propagating magnetic discontinuity.

Available data from the literature on the range in domain wall velocity in various materials are discussed and are compiled in tabulated form. Included are some results of experimental data obtained in this laboratory during the period of this contract.

Finally, several geometries are suggested for a suitable time delay system. In view of the high domain wall velocities, none of these systems are of use for time delays greater than several seconds.

TABLE OF CONTENTS

LIST OF TABLES

LIST OF FIGURES

INTRODUCTION

The first concept of a magnetic time delay device would embody the main features of the classical experiments conducted by Sixtus and Tonks. A long thin wire or tape of homogeneous magnetic material is placed in a long solenoid. The magnetization of the wire or tape is completely aligned axially by the solenoid field, H_s. When the main field is removed the magnetization must remain aligned, which requires the wire to have a longitudinal anisotropy. The main field is now reduced to zero, reversed, and increased to a value H, less than the axial anisotropy field 2K/M so that the original direction of magnetization is unchanged. A local pulse field H_p in the direction of the reversed main field is now applied near one end of the solenoid. If the pulse field plus the solenoid field exceeds a critical value H_o a nucleus of reversed magnatization is formed. The pressure exerted by the main field on the domain wall of the nucleus causes it to grow. When the wall reaches the wire surface, it splits into two mirror halves, each propagating in opposite direction to the ends of the wire, thus progressively reversing the magnetization in the wire.

One or more small sensing coils are would on the wire. The time delay is the elapsed time from the start of the pulse field until the domain passes through the sensing coils. The delay is adjusted by either changing the position of the sensing coil relative to the pulse coil, or changing the main solenoid field or both.

PROPERTIES OF THE MAGNETIC MEDIA WHICH AFFECT WALL MOTION

The range of wall velocity is controlled by the solenoid field, however the range is rather limited (see Figures 5 and 8). For low applied fields the dependency of velocity on field is linear and may be expressed as:

$$v = R(H - H_o) \qquad (1)$$

where R is the wall mobility constant, to be developed, H is the applied field, and H_o is the critical nucleating field. The difference $(H-H_o)$, exerts a pressure to move the wall, or in equivalence supplies the energy to all losses associated with wall motion.

There is both a lower and upper limit to the velocity for coherent wall motion. Below the lower limit the wall shape and area vary and it progresses in erratic jumps dependent on the local variation in structure of the magnetic media. Above the upper limit where the applied field now approaches the magnitude of the anisotropy field, 2K/M, nucleation may occur at random along the media, hence several walls may propagate simultaneously. If the field is further increased a state of non-uniform rotation of the magnetization takes place, this is the lower limit for fast switching devices. If the applied field exceeds the anisotropy field, reversal takes place by an almost simultaneous rotation of magnetization.[2]

In order to adequately discuss the factors which enter the wall mobility equation, a short summary is given of the energy and loss terms relevant to

the phenomena of wall motion. An appendix is included in which a brief development is given of the wall parameters for an ideal 180° wall. See the review articles given in Reference 3 for a more extensive development.

In the following energy density equations, constant terms which do not enter the wall equations are omitted.

The exchange energy density is given by:

$$f_{ex} = A[(\nabla \alpha_1)^2 + (\nabla \alpha_2)^2 + (\nabla \alpha_3)^2] \qquad (2)$$

where A is the exchange constant and the alphas are the direction cosines of the magnetization vector with respect to the principal axes of the cubic crystal. Equation (2) gives the energy per unit volume of interaction between an electron spin and its nearest neighbors which contribute to the magnetization. The energy is isotropic and has a minimum value when the spins are completely aligned. Values of A reported in the literature vary widely in different materials, however they are of the same order of magnitude. An average value of 2×10^{-6} ergs/cm^3 will be used here.

For a cubic crystal the crystalline anisotropy energy density is:

$$f_{an} = K_1[\alpha_1^2\alpha_2^2 + \alpha_2^2\alpha_3^2 + \alpha_1^2\alpha_3^2] + K_2[\alpha_1^2\alpha_2^2\alpha_3^2] \qquad (3)$$

which measures the energy required to rotate the magnetization from an easy to hard direction in the unstrained crystal. Positive anisotropy indicates the cube edges are the direction of easy magnetization. The anisotropy energy is extremely sensitive to temperature, changing at approximately the tenth of higher power of temperature, increasing as the temperature is lowered.

It also may vary as much as an order of magnitude depending on the state of order in the material. For permalloys at room temperature[4] K_2 is about 6 percent of the magnitude of K_1 and may be neglected. Values of K_1 range from 12 x 10^3 ergs/cm^3 for 40 percent nickel content to zero at 74 percent nickel (Ni_3Fe) in the quenched state. In permalloys which have been slowly cooled K_1 varies from 10 x 10^{-3} at 40 percent nickel, zero at 63 percent nickel to -25 x 10^3 at 74 percent nickel. The range for furnace cooled materials lies in between the above values. Uniaxial anisotropy may be induced by annealing in a magnetic field.[5] The induced anisotropy will vary from zero to 4 x 10^3 ergs/cm^3 dependent on the cooling rate. K_1 is taken to be -7 x 10^3 ergs/cm^3 for the .72 Ni - .28 Fe material investigated here.

The magnetoelastic or magnetostrictive energy density for the isotropic case, $\lambda_{100} = \lambda_{111} = \lambda$ is:

$$f_{me} = 3/2 \lambda T \sin^2 \beta \qquad (4)$$

where λ is the magnetostrictive strain constant, T the applied tensile stress, and β is the angle between the magnetization vector and the direction of applied stress. The magnetostrictive energy arises from the interaction between the magnetization and the mechanical strain of the crystal lattice. The energy is stored in the deformation strain of the lattice. Positive λ indicates the magnetization will have an easy direction in the direction of applied tension or perpendicular to an applied compressive stress. Both λ_{100} and λ_{111} are positive in the range from about 45 percent nickel to slightly less than 80 percent nickel and is independent of heat treatment

with the exception of the 68 to 80 percent range. For .72 Ni - .28 Fe, quenched state, the magnetostriction is nearly isotropic and λ is taken to be about 15×10^{-6}.[4]

Crystal anisotropy energy and magnetostrictive energy are closely related, the source of the latter being somewhat obscure. It is noted that a lattice of high symmetry has low anisotropy, and of low symmetry, high anisotropy as is evident from comparison of the respective values for iron and cobalt.

The magnetostatic energy density:

$$f = -\mu_o \bar{H} \cdot H \tag{5}$$

gives the interaction of the magnetization as a dipole with the applied field. $\bar{H}$ is taken as the effective field interior to the magnetic media, one component of which is the applied field.

The energy of the magnetization in its own field is:

$$f_s = \frac{\mu_o}{2} \bar{H}_d \cdot \bar{M} \tag{6}$$

where $\bar{H}_d$ is the demagnetizing field which arises when $\nabla \cdot \bar{M} \neq 0$. The demagnetizing field is a function of the shape of the magnetic media and the change in $\bar{M}$ through the media. Theoretically it may be calculated from:

$$\bar{H}_d = \frac{1}{4\pi} \int_{vol} (\bar{M} \cdot \nabla) \nabla \left(\frac{1}{|\bar{r}-\bar{r}'|} \right) dv \tag{7}$$

where $\bar{H}_d(r')$ and $\bar{M}(r)$, however the solution depends on a knowledge of $\bar{M}(r)$. The demagnetizing field may be most conveniently stated in terms of the de-

magnetizing factor

$$\bar{H}_d = - N \bar{M} \tag{8}$$

LOSS MECHANISMS

When a field is applied to a magnetic media, the magnetization changes in direction by rotation about the field. The loss accompanying the rotation is attributed to spin-spin and spin-lattice interactions of a complex nature. With loss the motion of precession about the applied field is damped and the magnetization motion decays exponentially toward the direction of the field. The process is given on a phenomenological basis by:[6]

$$\frac{\partial \bar{M}}{\partial t} = \gamma \bar{M} \times \left(\bar{H} - \frac{\alpha}{\gamma M} \frac{\partial \bar{M}}{\partial t} \right) \tag{9}$$

where

$\gamma = g \frac{\mu_o e}{2m}$; $\frac{ge}{2m}$ is the gyromagnetic ratio

$g \cong 2$, is the Lande factor

α = dimensionless loss factor.

This form, suggested by Gilbert, gives a damping term proportional to the time rate of change of magnetization and results in a minimum time of reversal for a finite value of the damping constant.

Due to the inertia of the spin system, the motion of magnetization in a moving wall will result in kinetic energy term proportional to the wall velocity squared. The inertia of the spin system summed through the moving wall is expressed as an equivalent wall mass, see appendix.

The change of magnetization with time in the moving wall induces an emf, and as a result eddy currents flow. The resultant power loss is a function of the shape of the domains and the magnetic material, conductivity, and wall velocity. The eddy current distribution is a boundary value problem, solved as follows:

$$\nabla^2 J = 0 \tag{10}$$

everwhere except within the wall. The boundary conditions are:

$$\bar{n} \cdot \bar{J} = 0 \tag{11}$$

at the conducting surface and

$$\pm \bar{n} \times \bar{J} = 2\mu_o \sigma M \bar{v} \tag{12}$$

at the wall surface. $\bar{n}$ is the unit outward normal at the media surface and at the domain wall respectively.

Both the relaxation damping of the magnetization and eddy current loss affect the wall mobility. Increase of α, the damping factor, and σ the conductivity decrease the wall mobility, thus for low wall velocity in a given field it is desirable to increase damping and conductivity.

Controlled domain wall motion is only observed in permalloy tapes above one eighth mil in thickness. In ferrites and very thin nickel-iron films or tapes relaxation damping is dominant and eddy current damping negligible.[7]

AXIAL PROPAGATION OF A DOMAIN WALL IN A FERROMAGNETIC CYLINDER

Since Sixtus and Tonks first studied the propagation of domain walls in permalloy wires, at least six other groups have extended the experiments (see References, 1, 8, 9, 10, 11, and 12). Extensive experimental data have been compiled on various compositions in the ranges of nickel composition from 10% to 20% and 40% to 80%. The data show variation of velocity with composition, heat treatment, cold work, tension and torsion; however little or no theoretical development was given. The first order analysis is due to Doring[13] and a brief review is given here with some modification.

The theoretical problem of the reversed domain nucleation, growth, and propagation may be approached rigorously by minimizing the total free energy of the magnetic configuration, with consideration of the loss terms. A variational solution would then yield the dynamic equations of motion of the magnetization. These equations may then be solved subject to the boundary conditions imposed at the media surface and through the moving region of magnetization reversal, as suggested by W. F. Brown.[14] The problem, however, is greatly complicated by two factors, namely: the demagnetizing field, Equation (7) and the retarding field produced by eddy currents. Both are a function of the magnetization spatial configuration in the zone of reversal and the magnetization configuration is dependent of these fields. The resultant equations are non-linear partial differential equations in space and time. No intensive effort has been made to solve these equations within the limited objective of this project, however they are of importance and a rigorous solution is required for a complete understanding of the problem.

A simplified approach requires a start from the experimentally determined shape of a reversed magnetic nucleus, and the assumption of an invariant shape as the reversed region grows to the media surface, thereafter propagating along the structure. Sixtus and Tonks[1] measured the shape of reversed magnetic region "frozen" in wires. When the nucleus region did not extend to the wire surface, it formed a prolate spheroid with the long axis parallel to the wire axis.

Doring[13] derived the critical ratio of major to minor axis for the nucleus which agreed well with experimental results. The assumption is made that the reversal nucleus exists as a uniformly magnetized prolate spheroid, separated from the surrounding magnetic media by a domain wall. Calculations from the integrated search coil voltage waveform show the shape of the moving discontinuity to be roughly one half of a spheroid with semi-minor axis equal to the wire radius; it is to be noted here that other shapes may be made to fit equally well but do not simplify the problem of the demagnetizing field. The ratio of semi-major axis to semi-minor axis is normally from 800 to 2,000. The lower figure applies to cold drawn permalloy wire, and is almost independent of wire diameter. Hydrogen annealed wires have an increase of the ratio from 900 to 2,000 as the wire diameter is decreased, as determined by the affect of the eddy current retarding field on the shape of the wall.

SHAPE OF THE REVERSED NUCLEUS AND MOVING WALL

Assume the magnetic media to be a long cylinder of radius a. The cylinder is initially fully magnetized to the right, see Figure 1. A field is applied axially to the left. At the center of the cylinder a domain will nucleate, which before it grows has an inner region uniformly magnetized to the left.

The energy of the nucleus is

$$U = \int_V 2\mu_o M(H - H_d)\, dv - \int_S \sigma_w\, ds \tag{13}$$

where reference is made to Equations (5) and (6) for the magnetostatic energy terms, and to the appendix Equation (43) for the wall energy term.

If the nucleus is to grow the applied field must exceed some critical value H_o, if less the nucleus will disappear, hence

$$d\,U \geqslant 2\mu_o M H_o\, dv \tag{14}$$

The demagnetizing energy term may be rewritten taking $H_x = -N_x M_x$, $H_z = -N_z M_z$, where N_x and N_z are the respective demagnetizing factors in the directions indicated. The energy density due to the demagnetizing field is

$$f_s = \int_o^{\pi} \mu_o(\bar{M} \times \bar{H}_d) \cdot d\bar{\theta} = -2\mu_o M^2 N_z \tag{15}$$

The reversed nucleus is taken to be a rotational spheroid with semi-minor axis c, semi-major axis b, with $b >> c$. The demagnetizing factor for this shape is:

$$N_z = \frac{1}{k^2}\,[\ln(2k) - 1] \tag{16}$$

Where $k = b/c \geqslant 500$, thus (16) is a very good approximation for N_z.

The total energy for the nucleus may be approximated now by:

$$U = \frac{8\pi}{3} c^2 b \mu_o HM - \sigma_w \pi^2 cb - \frac{8\pi}{3} \mu_o M^2 \frac{c^4}{b} [\ln(2k) - 1] \tag{17}$$

The critical length of the nucleus with respect to a given radius is found by differentiating the total energy with respect to b, and then placing this result in (14) using the equal sign. From (14):

$$\frac{\partial U}{\partial b} = \frac{8\pi}{3} \mu_o H_o M c^2 \tag{18}$$

The result of this operation after some rearrangement is:

$$\frac{\ln(2k) - 2}{k^2} = \frac{\frac{3\pi\sigma_w}{c} - 8\mu_o M(H - H_o)}{8\mu_o M^2} \tag{19}$$

If H exceeds H_o for a given radius c, the nucleus will continue to grow. When c = a, the radius of the cylinder, the surface of the nucleus on merging with the boundary splits into two sections of length b. Each section propagates in opposite directions at a velocity determined by $(H-H_o)$.

The shape of the propagating domain wall is now considered to be one symmetric half of a prolate spheroid. The applied field less the critical field must now supply the eddy current and damping losses. The energy integral is taken over the volume containing the region of the propagating wall, since the magnetization in the remainder of the cylinder is stationary.

The true shape of the wall in motion has a greater slope at the cylinder boundary and less slope along the lateral surface than is given by the above assumed shape.

Nucleation, in reality, may occur anywhere in the volume of the media inside the pulse coil. Two or more nuclei may form, not necessarily simultaneously, grow, merge, then propagate along the wire. Since the pulse coil has a short rise time, eddy currents induced by the pulse field delay the penetration of the field into the wire, thus it is more probable that a nucleus be formed near the surface rather than at the center of the wire. The nucleus would spread over the wire surface and then penetrate to the center, where it would then break into two sections moving in opposite directions with the tip at the center trailing. The general shape of the wall is approximately the same whether the tip leads or trails in motion. Either type of motion is equally probable.

INDUCED VOLTAGE AND EDDY CURRENT DAMPING

The solution for the eddy current loss would proceed as outlined in Equation (10) through (12), however the circular symmetry of the domain wall allows a more direct approach. Since the length to radius ratio of the wall is greater than 500, the wall is taken to have a conic shape as shown in Figure 2. The equation of the domain wall is now simply $x = k\,z$, $k = b/a$ and the coordinates are moving with the wall at velocity v. The voltage induced in any path circularly concentric with the wire center is:

$$V = \frac{4\pi\mu_o M_z v}{k^2} \qquad \text{for } r > x$$

$$V = 0 \qquad \text{for } r < x \qquad (20)$$

Equation (20) gives the voltage per turn induced in any coil wound about the wire.

The voltage gradient is θ directed, and constant along any circular path of radius r, from (20)

$$E_\theta = \frac{2\mu_o Mvz}{k^2 r} ; \qquad r \geqslant x \tag{21}$$

The eddy current power loss is found by integrating σE_θ^2 through all the volume of conducting media outside the domain wall and over the length $0 \leqslant z \leqslant b$.

Inside the wire

$$P_e = 2\pi\sigma \int_o^\lambda \int_x^a E_\theta^2 \, r dr dz \tag{22}$$

which reduces to

$$P_e = \left(\frac{4\pi\mu_o Mv}{k^2}\right) \frac{\sigma b^3}{18\pi} \tag{23}$$

The power loss ina surrounding conducting tube of inside radius a_1, outer radius a_2, and conductivity σ_2 is from (22) changing the limits on x from a_1 to a_2:

$$P_e = \left(\frac{4\pi\mu_o Mv}{k^2}\right)^2 \frac{\sigma_2 b^3}{6\partial} \ln\left(\frac{a_2}{a_1}\right) \tag{24}$$

The power input of the applied field is:

$$P = 2\mu_o M H_e \pi a^2 v \tag{25}$$

Equating the sum of (23) and (24) to (25) gives, after simplification:

$$v = \frac{9bH_e}{4\mu_o Ma^2\sigma[1 + 3\frac{\sigma_2}{\sigma}\ln\left(\frac{a_2}{a_1}\right)]} \tag{26}$$

or the mobility due to eddy currents alone is:

$$R_e = \frac{9b}{4\mu_o Ma^2\sigma[1 + 3\frac{\sigma_2}{\sigma}\ln\left(\frac{a_2}{a_1}\right)]} \tag{27}$$

Where the second term in the denominator of (27) gives the contribution of an eddy current damping tube to decrease the mobility.

Assuming the wall to be one half of a rotational ellipsoid, the equation for the voltage induced in a circular path is unchanged, however instead of Equation (27), the mobility becomes

$$R_e = \frac{.39b}{\mu_o Ma^2\sigma[1 + .52\frac{\sigma_2}{\sigma}\ln\left(\frac{a_2}{a_1}\right)]} \tag{28}$$

From a comparison of (27) and (28) it is evident that the ellipsoid wall results in a mobility of only 17 percent of that for the conic wall. The exact mobility cannot be determined until a more proper equation for the wall shape is found. The formal significance of these equations, since they are dimensionally correct, is the manner in which conductivity, magnetization, and wire size affect mobility.

The eddy current mobility may be expressed more generally:

$$R_e = \frac{b}{4\mu_o Ma^2\sigma f[1 + \frac{3}{f}\frac{\sigma_2}{\sigma}\ln\left(\frac{a_2}{a_1}\right)]} \tag{29}$$

where:

$f = .111$, conic wall

$f = .64$, half rotational ellipsoid wall

WALL DAMPING DUE TO RELAXATION LOSS

The total loss due to spin relaxation processes cannot be given with any accuracy until a better model of the shape of moving wall is developed. This loss is dependent on knowledge of the spin angular variation through the wall which is unknown in detail. However the power loss per unit of wall area should be of the same form as for a plane wall, thus the total loss will be given to a first order only in terms of a dimensionless constant proportional to the cross sectional area of the wire, inversely proportional to the area of the domain wall, let this constant be q, then in terms of Equation (49)

$$R_r = q\delta\gamma\left(\frac{1+\alpha^2}{\alpha}\right) \tag{30}$$

This at least shows the factors which control relaxation damping mobility.

GENERAL EQUATION FOR WALL VELOCITY

From the definition of the wall mobility, as derived from the force equation, see appendix

$$v = \frac{2\mu_o M}{B}(H - H_o) \tag{31}$$

where $H-H_o$ is the field which supplies the loss as the wall moves.

The total mobility term, considering eddy current, and relaxation is determined then from the reciprocal relation; since B_r and B_e are additive, or

$$R^{-1} = R_e^{-1} + R_r^{-1} \tag{32}$$

The final wall equation becomes

$$v = R[H - H_o] \tag{33}$$

where R_e and R_r are given by Equations (29) and (30) respectively.

As an example of the relative contribution of eddy current and relaxation damping to the mobility, data were taken from a run on a .72 Ni - .28 Fe wire .0114 cm diameter, see Figure 8. The experimental data are as follows:

$T = 58.7 \text{ kg/mm}^2$

$R = 19{,}500 \text{ cm/sec-oe}$

or

$R = 2.45 \text{ mks}$

$b = 4.85 \text{ cm}$

$k = 850$

Using the data given in Table IV and Equation (29), the eddy current mobility is:

$R_e = 9.37 \text{ mks, conic wall}$

$R_e = 1.62 \text{ mks, ellipse wall}$

From (32), the relaxation mobilities are:

R_r = 3.32 mks, conic wall

R_r = negative value, ellipse wall

The conic wall gives a realizable relaxation term; that for the elliptic wall is not realizable, hence the wall shape is probably intermediate between these two extremes.

The anisotropy constant due to applied tension is 2.58×10^5 ergs/cm^3 or at least 100 times the crystalline anisotropy energy. The wall which parameter $\delta = 2.8 \times 10^{-6}$ cm or several hundred lattice constants.

FACTORS CONTROLLING WALL MOTION

The material parameters which determine the wall velocity are evident from an inspection of the mobility Equations (29) and (30); however, since these factors add reciprocally to give the net inverse mobility, it is more convenient to look at the gross damping factor B, from Equation (31):

$$B = \frac{\mu_o M \alpha}{q\delta (1 + \alpha^2)} + \frac{(2\mu_o M)^2 \, 2a^2 \, \sigma f}{b} \left[1 + \frac{1}{3f} \frac{\sigma_2}{\sigma} \ln \left(\frac{a_2}{a_1} \right) \right] \qquad (34)$$

where:

f = .111, conic wall

f = .64, elliptic wall

All material parameters in (34) increase with a decrease of temperature. The axial wall length increases with decrease in temperature as seen from Equation (19). The combined effect is to increase B, hence decrease the

mobility by lowering the temperature. The critical field H_o also increases as temperature drops. The mobility in a nickel ferrite crystal at room temperature is 150 times the value at liquid nitrogen,[17] the change in the range of room temperature is less than 10 percent. The mobility increases from 42 cm/sec-oe at 10°C to 58 at 95°C in .60 Ni - .40 Fe permalloy, see Tables I and III. Since both mobility and critical field are temperature sensitive, temperature control is a requirement for constant delay time.

The field difference for low field wall motion is normally less than an oersted, since stray fields may easily exceed this value, shielding is necessary.

The final important requirement for uniform wall motion is a high uniaxial anisotropy in the direction of wall motion. If the magnetization is not aligned, wall shape and velocity have high local variations, thus time delays are not reproducible and pulse voltages are variable. Uniaxial anisotropy is brought about in three ways:

(a) High percent reduction in cross section by drawing or rolling. The residual stress due to plastic elongation in the roll direction produces a net uniaxial anisotropy in this direction with positive magnetostriction, transverse if the magnetostriction is negative. The alignment varies through the cross section, being very poor near the lateral surfaces.[23]

(b) Alignment of the easy axis of the crystallites in the axial direction by anneal in a magnetic field.[5] Uniaxial alignment of magnetization is low in soft cubic magnetic materials.

(c) Tension in the axial direction for materials with positive magnetostriction. Compression or combined tension and torsion with negative magnetostriction. Optimum stress is just below the elastic limit.[22]

No single method produces an ideal alignment. The combination of the above three techniques in the order listed produces the best condition for uniform wall motion, however the mobility is extremely high -- up to 78,000 cm/sec-oe. A permalloy baked for about an hour in hydrogen, quenched in air, then stressed to just below the elastic limit yielded a sample with uniform wall motion, and the mobility was reduced to 14,000 cm/sec-oe. The addition of an eddy current damping tube to this sample further reduced the mobility to 7,500 cm/sec-oe. In comparison a cold drawn sample of the same material, when placed in the same eddy current tube, resulted in a reduction in mobility from 13,500 to 3,500 cm/sec-oe, however the wall motion is erratic. The above data were taken with a .60 Ni - .40 Fe wire, .005 cm radius.[10]

The following discussion refers to data obtained during the period of this contract. Figures 4 through 10 show results obtained on .72 Ni - .28 Fe wire using the experimental setup shown in Figure 3. The propagating field was measured with a d-c digital voltmeter to within ±3 percent. The pulse and saturation fields were measured on an oscilloscope to within ±10 percent. All fields have been corrected for the ambient field which averaged from .45 to .50 oersted along the solenoid axis.

The wire was obtained from the Driver-Harris Company, Harrison, N. J. After cold reduction to the required size, the wire is baked in a hydrogen

atmosphere, then air quenched to room temperature. The samples were unfortunately subjected to sharp bends on shipment, which resulted in erratic wall motion at low tension. After a slight plastic set wall motion became very uniform over the linear range of propagation.

A comparison of Figures 5 and 6 show the effect of added eddy current damping on wall mobility. The .020 diameter wire was placed in a .320 by .158 cm diameter brass tube which decreased the mobility by over 50 percent for the same tension. These two graphs are not a good means of comparing the change in driving field with the addition of the damping tube. The data for Figure 5 were taken subsequent to the removal of the conducting tube, after which the wire was given an extreme plastic set, hence the large increase in H_o.

The effect of tension on mobility and H_o for an initially unstrained sample is illustrated in Figure 9a. Both mobility and H_o reach a minimum just below the elastic limit. After plastic set H_o increases but R remains less than the initial value due to the residual strain. In Figures 7 and 10 are shown the hysteresis in mobility and H_o with change in tension after plastic set. These curves are reproducible in samples subjected to the same degree of plastic stretch.

A comparison of Figures 5 and 8, or 7 and 10, show the increase in wall mobility with decrease in wire radius. The ratio of wire areas is 3.18, the ratio of mobilities at 50 kg/mm^2 tension is 0.80, which compares favorably with the respective ratios predicted from Equation (34).

Figure 11 shows the motion of walls caused by reverse domains nucleated

at the ends of a wire extending beyond the drive field solenoid. End nucleation may be minimized by termination within the region of uniform drive field. The termination should be designed so as not to increase the tension stress over that in the wire proper, or introduce torsional stress.

Tension induced anisotropy did not give complete alignment of the magnetization. The B-H loops taken for the wire under tension are square, with a maximum magnetization of 7,200 gauss at all tensions above 2.1 kg/mm^2. The maximum drive field was 6 oersted, the coercive field was 2.8 oe. The coercive force shows little or no relation to H_o, the latter being quite sensitive to strain. The saturation magnetization at room temperature is 12,000 gauss, or only 60% of the magnetization is axially reversed by the wall motion. Calculations of eddy current damping and induced voltage in sense coils should use the switched magnetization ΔM rather than magnetization M.

Two permalloy tapes were tested but no uniform axial wall motion was found. The tapes were 1/8 mil by 1/16 inch in cross section, and were cold worked with no subsequent anneal. The .50 Ni - .50 Fe tape under high pulsed field exhibited random nucleation and wall motion across the tape.[24] The 4-79 Mo permalloy tape broke before sufficient tension was applied. The latter material has low magnetostriction and conductivity, neither conducive to uniform axial wall motion.

Both tapes had extremely rough edges due to slitting. The edge roughness probably caused local regions with a closure domain structure, which was not removed by the saturation field. These regions are nucleation points

for walls which move across the tape width when the drive field is applied. A non-uniform strain distribution was quite noticeable across the tape width which was probably due to residual strain induced during cold rolling. This would be removed by heat treatment. Non-uniformity of axial wall motion appears to exist even in annealed tapes as evidenced by the mobility data in Table II for .48 Ni - Fe permalloy. For the same cross sectional area the wall mobility in a thin tape will be considerably higher than in the wire since the tape geometry lowers the eddy current contribution to the damping.

DESIGN OF A MAGNETIC TIME DELAY SYSTEM

In summary, the following criteria should be considered:

(a) The magnetic media should be in a long filament geometry, probably circular in cross section rather than rectangular for the reasons noted above. The long, small cross section configuration gives a minimum demagnetizing factor in the preferred axial direction of magnetization.

(b) The material, since it is polycrystalline, must have high induced axial anisotropy. Crystal anisotropy should be low and magnetostriction high, however the two are uniquely related, so a compromise is necessary. The .48 to .79 percent nickel content permalloys show a decrease in both quantities as the nickel content is increased. Probably a composition near 60% nickel is best since the magnetostriction is nearly isotropic, and the crystal anisotropy very low in the ordered state.

(c) The wire should be stressed to a point just below the elastic limit, and the structure designed to maintain constant stress.

(d) Reverse saturation and driving fields must be very uniform along the axis of propagation.

(e) The magnetic wire must be well shielded from stray fields.

(f) A conductive eddy current envelope may be used to lower wall mobility.

(g) Some means of temperature control is required to maintain constant mobility.

For a one shot time delay d-c supplies may be used. The wire must be initially saturated opposite to the direction of wall motion. To initiate the time delay, the saturation current circuit is opened and simultaneously the reverse domain coil circuit and drive field circuit are energized. Repetitive time delays can only be generated by pulsing the saturation solenoid and nucleation coil.

The maximum time delay is small. With reference to Figure 6, the lowest mobility is 4,200 cm/sec-oe, and the lowest velocity is slightly below 2,000 cm/sec. This corresponds to a delay of 50 milliseconds per meter. Long delays can only be realized by use of extremely long lengths of wire. Long time delays in a small package seem improbable in the light of the above restrictions.

The following structures are suggested for a magnetic time delay device:

(a) The twister geometry appears favorable subject to the requirement of precisely controlled tension along the magnetic wire. This structure

simplifies the problem of obtaining a uniform driving field along the wire. A model has been built here, but not tested. The scale is large: a 1/8 inch center conductor wrapped with a helix of .020 permalloy wire. The objective here is to determine whether the stressed wire relaxes with time, if so, to what extent the wall velocity is changed.

(b) The magnetic wire is wound under tension helixally over the surface of a thin walled rigid plastic tube. The saturation and drive field windings are wound as toroidal coils over the magnet wire. For a one shot delay the current sources may be packed inside the tube.

(c) An intriguing configuration should be mentioned. A thin uniform layer of permalloy, having negative magnetostriction is plated or bonded on a conducting wire.[25] Permalloy with a nickel content exceeding 85 percent is suitable. When the wire is placed under tension the easy direction of magnetization is circumferential. The saturation and driving fields are produced by currents flowing through the conducting core. The nucleation coil is wound over the surface of the magnetic layer in a skewed manner so as to create a local field reversing the magnetization in the circumferential direction. The circular wall now moves down the structure at a velocity determined by the driving field. This is an ideal geometry since the demagnetizing field in the easy direction is zero. The principal drawback appears to be obtaining uniform properties in the magnetic layer.

(d) Another device based on a different principal may prove useful. This is the thin magnetic film shift register developed by Broadbent and McLung.[26] A strip of thin film or tape is placed between axially displaced

pump windings. These windings are pulsed alternately to form a pump field which progressively travels along the magnetic strip. The pulse frequency controls the field velocity. The strip is first saturated in the direction opposite to pump field motion. The saturation field is removed and a reversed domain nucleated near one end of the strip. The pump field now forces the reversed domain to progressively jump along the strip. The length of time delay is only limited by the gradual degeneration in shape of the reversed domain as it moves along the tape.

Several other structures may be suggested, however the requirements of constant tension and uniform drive field immediately narrows the field to the four described. Structures (b) and (c) should be the basis of further development work necessary to realize a compact magnetic time delay device.

APPENDIX

THE 180° MAGNETIC DOMAIN WALL

Expressing Equation (2) through (6) for the free energy density terms in spherical coordinates:

$$f_{ex} = A[(\nabla\theta)^2 + \sin^2\theta\,(\nabla\phi)^2] \tag{35}$$

$$f_{an} = \frac{K_1}{4}[\sin^2 2\theta + \sin^4\theta \sin^2 2\phi] + K_m \sin^2\beta \tag{36}$$

$$f_h = -\mu_o\overline{M}\cdot(\overline{H} - \overline{H}_d) \tag{37}$$

The angle θ gives the orientation of $\overline{M}$ with respect to a z axis, and $\overline{M}\sin\theta$ subtends the angle ϕ with the x axis in a right handed xyz coordinate system. Equation (36) gives the sum of magnetocrystalline and strain induced anisotropy energy, where $K_m = \frac{3}{2}\lambda T$, and β is the angle between the applied tension stress and the magnetization.

With no field applied the magnetization exists in a state of equilibrium which may be found by minimizing the total free energy of the ferromagnetic body.

From experimental observation it is found that the static state of magnetization exists as uniformly magnetized domains oriented parallel to the direction of least anisotropy energy. Near crystal surfaces or non-magnetic inclusions, closure domains form to minimize the self magnetostatic energy, hence the gross domain configuration is determined by the size and shape of the magnetic body and size, shape, and spatial orientation of the

crystals which compose the body.

The regions between adjacent uniformly magnetized domains -- the domain walls, are relatively thin in comparison to the thickness of the bounding domains. The walls seek an orientation to minimize the anisotropy, exchange and magnetostatic self energy due to the spatial variation of magnetization separating the uniformly magnetized regions. An exact minimum energy configuration is not theoretically determinable by simply assuming domain walls and drawing in the proper closure domains, but at least this process leads to one of several realizable configurations. The possible wall orientations which may exist in a single crystal is determined by the anisotropy energy,[27] only the simple 180° plane wall is considered here.

Consider an infinite wall in the x-y plane, with a tensional stress applied in the x direction. The adjacent domains are aligned with $\overline{M} = +M_x$, $z = -\infty$, $\overline{M} = -M\ x$, $z = +\infty$. The applied field is zero and only a ϕ variation is allowed, hence the demagnetizing field normal to the wall is zero. The free energy per unit area in the volume of a cylinder normal to the wall is:

$$\sigma_w = \int_{-\infty}^{\infty} f dz \tag{38}$$

where the energy density f is given by the sum of Equations (35) and (36). The state of minimum energy is found by applying the variational operator

$$\frac{d}{dz}\left[\frac{\partial f}{\partial\left(\frac{\partial \phi}{\partial z}\right)}\right] - \frac{\partial f}{\partial \phi} = 0 \tag{39}$$

to the total free energy density, subject to the condition that the variation is zero at $z = \pm \infty$. The result is:

$$2A \frac{\partial^2 \phi}{\partial z^2} - \frac{\partial\, fan}{\partial \phi} = 0 \tag{40}$$

which states that the torques exerted by the anisotropy and exchange fields on the magnetization are equal and opposite through the wall.

Multiplying by $d\phi$ and integrating gives:

$$\frac{\partial \phi}{\partial z} = \left| \frac{fan}{A} \right|^{1/2} \tag{41}$$

Solving (41) for the wall thickness:

$$z = \delta \ln \left[\frac{\tan \phi}{\left(1 + \frac{K_1}{K_m}\right)^{1/2} + \left(\frac{K_1}{K_m} + \sec^2 \phi\right)^{1/2}} \right] \tag{42}$$

where $\delta = \left(\frac{A}{K_1 + K_m}\right)^{1/2}$ is the wall thickness parameter. Mathematically the wall has an infinite thickness, however most of the angular variation takes place in a width of 10 δ normal to the wall.

The wall energy per unit area is found by inserting (41) and (42) in Equation (38) and integrating:

$$\sigma_w = 2[A(K_1 + K_m)]^{1/2} \left\{ 1 + \frac{\frac{K_m}{K_1}}{\left(1 + \frac{K_m}{K_1}\right)^{1/2}} \tanh^{-1} \left(1 + \frac{K_m}{K_1}\right)^{1/2} \right\} \tag{43}$$

Let an external field be applied in the x direction parallel to the wall in an x-y plane. If the field is much less than the anisotropy field, 2K/M, the magnetization within the domains remain respectively parallel and

antiparallel to the field. In the intervening wall, however, the magnetization is at an angle ϕ with respect to the field and experience a torque which causes it to start a precession about the applied field. There results a component of magnetization normal to the wall surface. Since $\nabla \cdot \overline{B} = 0$ always, a demagnetizing field H_e[28] is formed perpendicular to the wall which is much greater than the applied field. The magnetization within the wall, thus perturbed by the low applied field now precesses about the field H_e at an angular velocity γH_e. The wall region moves parallel to its normal in the direction of the domain aligned antiparallel to the field. The spin angular distribution within the moving wall is essentially the same as within the wall at rest, hence

$$\phi = f(z - vt)$$

and

$$\frac{\partial \phi}{\partial t} = - v \frac{\partial \phi}{\partial z} = \gamma H_e$$

or

$$H_e = - \frac{v}{\gamma} \frac{\partial \phi}{\partial z} \qquad (44)$$

The energy density within the wall associated with H_e is $\frac{\mu_o H_e^2}{2}$ which is proportional to the square of the wall velocity. This term is a measure of the additional energy stored in the inertia of the spin system of the moving wall volume, and is conveniently expressed as the kinetic energy of an equivalent wall mass[29] per unit area:

$$\frac{mv^2}{2} = \int_V \frac{\mu_o H_e^2}{2} \, dv.$$

Integration over a cylinder of unit area and infinite length normal to the wall, using Equation (44) gives:

$$m = \frac{\mu_o}{\gamma^2} \int_{\delta}^{\pi} \left| \frac{\partial \phi}{\partial z} \right| d\phi \tag{45}$$

Substitution of Equation (41) into (45) gives the wall mass:

$$m = \frac{\mu_o}{\gamma^2 \delta} \left[1 + \frac{\frac{K_m}{K_1}}{\left(1 + \frac{K_m}{K_1}\right)^{1/2}} \tanh^{-1} \left(1 + \frac{K_m}{K_1}\right)^{1/2} \right] \tag{46}$$

For either $K_1 = 0$ or $K_m = 0$, Equation (46) simplifies to:

$$m = \frac{\mu_o}{\gamma^2 \delta} \tag{46a}$$

The power loss per unit of wall area due to relaxation damping is equivalent to a gross viscous damping loss $\frac{Bv^2}{2}$. From Equation (9), making use of the fact that H_e is much greater than the applied field, the power loss per unit volume in the wall is:

$$\mu_o \bar{H} \cdot \dot{\bar{M}} = \frac{\mu_o \alpha \gamma M H_e^2}{\alpha^2 + 1} \sin^2 \phi \tag{47}$$

Integrating over a cylinder of unit area, and infinite length normal to the wall gives the power input per unit area necessary to supply the loss. From Equation (47) and (44):

$$2\mu_o M H_r v = \frac{\mu_o \alpha M v^2}{(\alpha^2 + 1)\gamma} \int_o^{\pi} \left(\frac{\partial \phi}{\partial z} \right) \sin^2 \phi d\phi \tag{48}$$

Substitution of Equation (41) into (48) after integration and rearrangement gives the gross viscous damping factor:

$$B = \frac{2\mu_o \alpha M}{\gamma(\alpha^2+1)\delta}\left\{-\frac{1}{2}\left(1+\frac{K_m}{K_1}\right)+\left(1+\frac{K_m}{4K_1}\right)\left[1+\frac{\frac{K_m}{K_1}}{\left(1+\frac{K_m}{K_1}\right)^{1/2}}\tanh^{-1}\left(1+\frac{K_m}{K_1}\right)^{1/2}\right]\right\} \quad (49)$$

For $K_1 \gg K_m$, Equation (49) simplifies to:

$$B = \frac{2\mu_o \alpha M}{\gamma(\alpha^2+1)\delta} \cdot \frac{1}{2} \quad (49a)$$

and for $K_m \gg K_1$ to:

$$B = \frac{2\mu_o \alpha M}{\gamma(\alpha^2+1)\delta} \cdot \frac{4}{3} \quad (49b)$$

General Equation of Wall Motion:

For a plane 180° domain wall with the field applied parallel to the wall, the differential equation of motion is:

$$M\ddot{z} + B\dot{z} + \alpha z = 2\mu_o MH \quad (50)$$

The (αz) term is the force which restrains the wall to the initial static equilibrium position. The term is assumed linear and lossless for motion of the wall over short distances. For wall motion over a large distance the term varies with the wall position and represents an irreversible loss, due to lattice inperfections and non-magnetic inclusions. The loss involved in this term has not been placed on a satisfactory quantitative basis and is not accounted for here. (See Reference 3a page 545 for additional detail.)

With a constant field applied, since the wall mass is small, the wall almost immediately reaches a constant velocity. The equation of motion may be more conveniently written as:

$$v = \frac{2\mu_o MH}{B} - \left\langle \frac{\alpha z}{B} \right\rangle$$

or finally, for low fields

$$v = R[H - H_o] \tag{51}$$

where

$$R = \frac{2\mu_o M}{B} \tag{52}$$

$$H_o = \left\langle \frac{\alpha z}{B} \right\rangle \tag{53}$$

R is the wall mobility, which is a constant for applied fields much less than the effective anisotropy field 2K/M. H_o is an average measure of the domain wall stiffness α over the distance it moves. Both terms, R and H_o, show minor variation as noted by repeated measurement of wall velocity vs. applied field under identical conditions of wall propagation.

TABLE I

DATA ON DOMAIN WALL MOTION IN PERMALLOYS AT LOW FIELD

Composition	State	Tension kg/mm^2	Velocity Range cm/sec x 10^{-3}	H x 10^{-3} cm/sec-oe	H_o oe	Diameter cm	Temp. °C	Ref.
.14 Ni - Fe	Cold drawn	38	2.5 - 10	25	5.4	.038	20 - 30	1
		46	2.5 - 20	28	5.0			
		62	3.0 - 15	32	4.6			
		92	3.0 - 15	20	3.4			
.10 Ni - Fe	Cold drawn	30	3.0 - 9.0	19	3.7	.0334	20 - 30	9
		42	3.0 - 12	19	3.3			
.50 Ni - .50 Fe	Annealed	4.8	13.0 - 24	47	0	.01	20 - 30	10
		8.8	8.0 - 24	42	.09			
		12.8	5.0 - 20	42	.17			
.60 Ni - .40 Fe	Annealed	4.8	3.5 - 10	28	.19	.01	20 - 30	10
		8.8	3.5 - 10	31	.23			
		12.8	3.5 - 10	30	.31			
.60 Ni - .40 Fe	Annealed	-	-	14.4	.11	.005	- 180	10
			-	42.2	.05		10	
			-	58.0	.05		95	
.60 Ni - .40 Fe	Cold drawn	30 - 80	-	12	-	.01	20 - 30	10
.60 Ni - .40 Fe	Cold drawn	-	-	4.2	3.36	.005	-180	10
			-	11.9	2.44		10	
			-	16.2	2.22		95	

TABLE II

DATA ON DOMAIN WALL MOTION IN .48 Ni - Fe TAPES
(Ref. 12)

State	T mil	W mil	H_o oe	b cm	R x 10^{-3} cm/sec-oe
Cold rolled	1	100	4.1	20 ± 3	17 ± 1
Cold rolled	1	40	4.5	9 ± 2	22 ± 1
Cold rolled	1/8	100	6.1	7 ± 2	9 ± 3
Annealed	1	100	0.35	50 ± 20	140 ± 20
Annealed	1	40	0.48	20 ± 3	170 ± 20
Annealed	1/8	100	0.31	16 ± 5	120 ± 30

TABLE III

DATA ON DOMAIN WALL MOTION IN SINGLE CRYSTALS

Composition	H_o oe	R cm/sec-oe	Velocity Range cm/sec	Temp. °K	Type Wall	Ref.
.04 Si - Fe	-	3.8	-	85	(100)	15
		4.7	-	180		
		5.4	-	290		
Fe_3O_4	.06	1,900	100 - 850	-	(110)	16
$(NiO)_{.91}(FeO)_{.09}Fe_2O_3$	1.5	20,000	-	-	(110)	16
$(NiO)_{.75}(FeO)_{.25}Fe_2O_3$	.075	26,160	0 - 6,000	201	(110)	17
$Mn_{1.4}Fe_{1.6}O_4$	1.4	94	0 - 500	77	(112)	19
	.015	805	160 - 370	77	(110)	
5.4μ x 10μ Fe Whisker	0^+	2,500	100,000 - 200,000	77	(100)	20
	0^+	7,000	100,000 - 400,000	200		
	0^+	8,000	100,000 - 500,000	298		

TABLE IV

PHYSICAL DATA FOR .72 Ni - .28 Fe PERMALLOY

Values are for the temperature range of 25 - 30°C

Magnetostriction constant: (assumed to be isotropic)

$$\lambda \cong 15 \times 10^{-6}$$

Crystal anisotropy energy: ergs/cm^3

$K_1 = 2 \times 10^3$ quenched

$K_1 = -7 \times 10^3$ furnace cooled

$K_1 = -20 \times 10^3$ slowly cooled

$K_2/K_1 < .06$

Exchange constant: ergs/cm

$$A \cong 2 \times 10^{-6}$$

reported values range from 1.6×10^{-6} to 3.3×10^{-6}.[29]

Relaxation damping constant: dimensionless

$0.3 < \alpha < 9$ dependent on frequency temperature, and technique of measurement.

Magnetization: gauss

saturation: $4\pi M_s = 12{,}000$

from B-H curves $4\pi M = 7{,}200$

Conductivity: mhos/cm

permalloy, $\sigma = 5.02 \times 10^4$

brass tube, $\sigma = 14.9 \times 10^4$

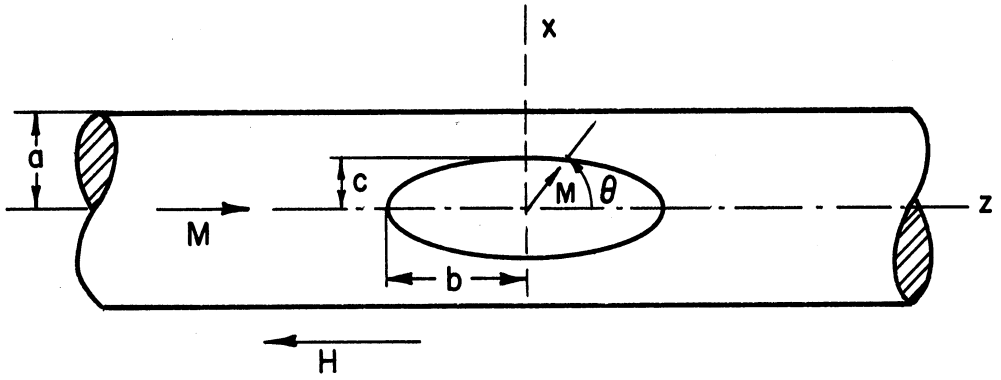

Fig. 1. Nucleation of a reversed domain in a uniformly magnetized cylinder.

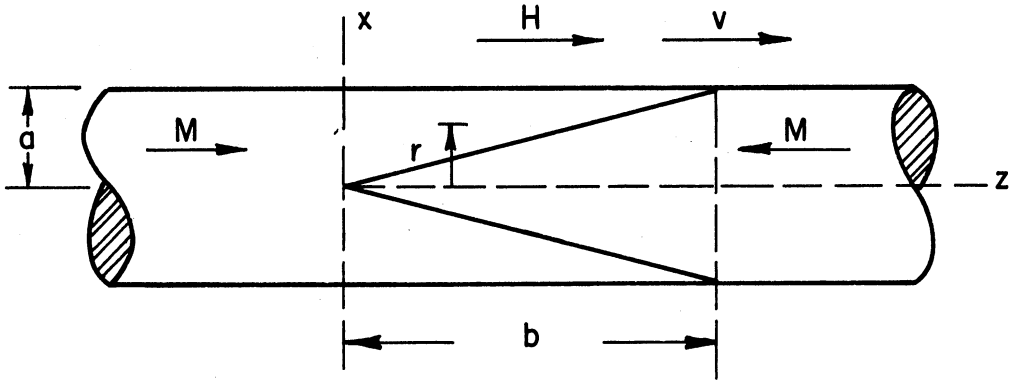

Fig. 2. Domain wall shape used for calculation of eddy current damping.

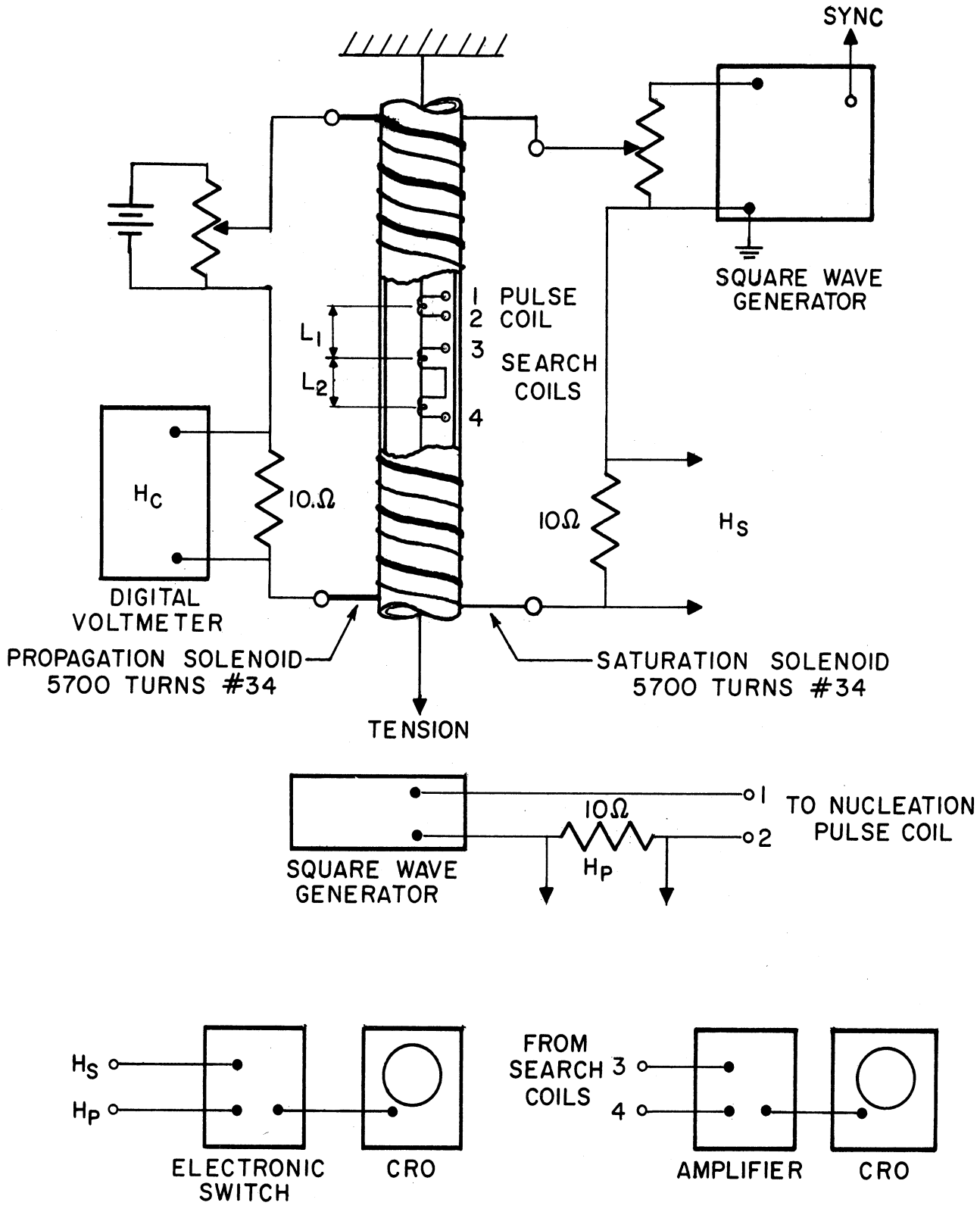

Fig. 3. System for measurement of wall velocity.

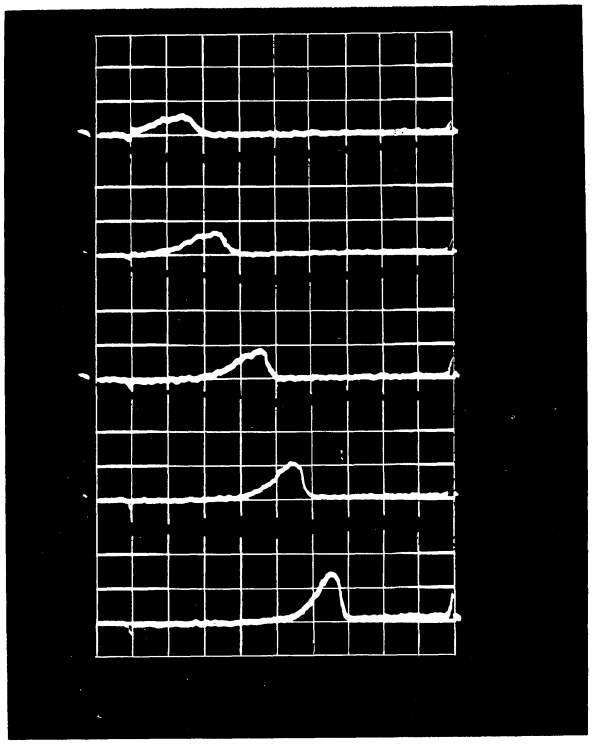

(a) .0203 cm diam. in a brass tube
L = 10 cm, T = 42.8 kg/mm^2
Scale: .23 mv/cm x 1 ms/cm

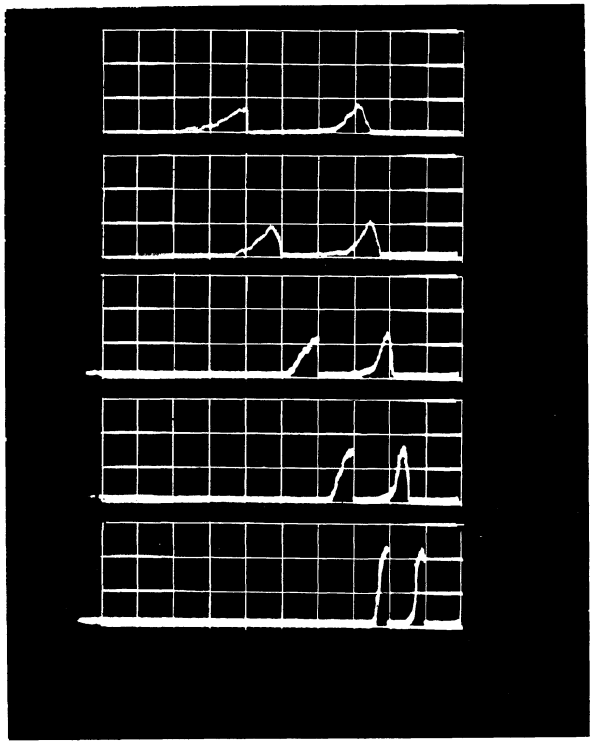

(b) .0114 cm diam.
T = 58.7 kg/mm^2, L = 10 cm
Scale: .5 mv/cm x 1 ms/cm

Time is measured from the right

Fig. 4. Output voltage of search coils wound on the permalloy wire.

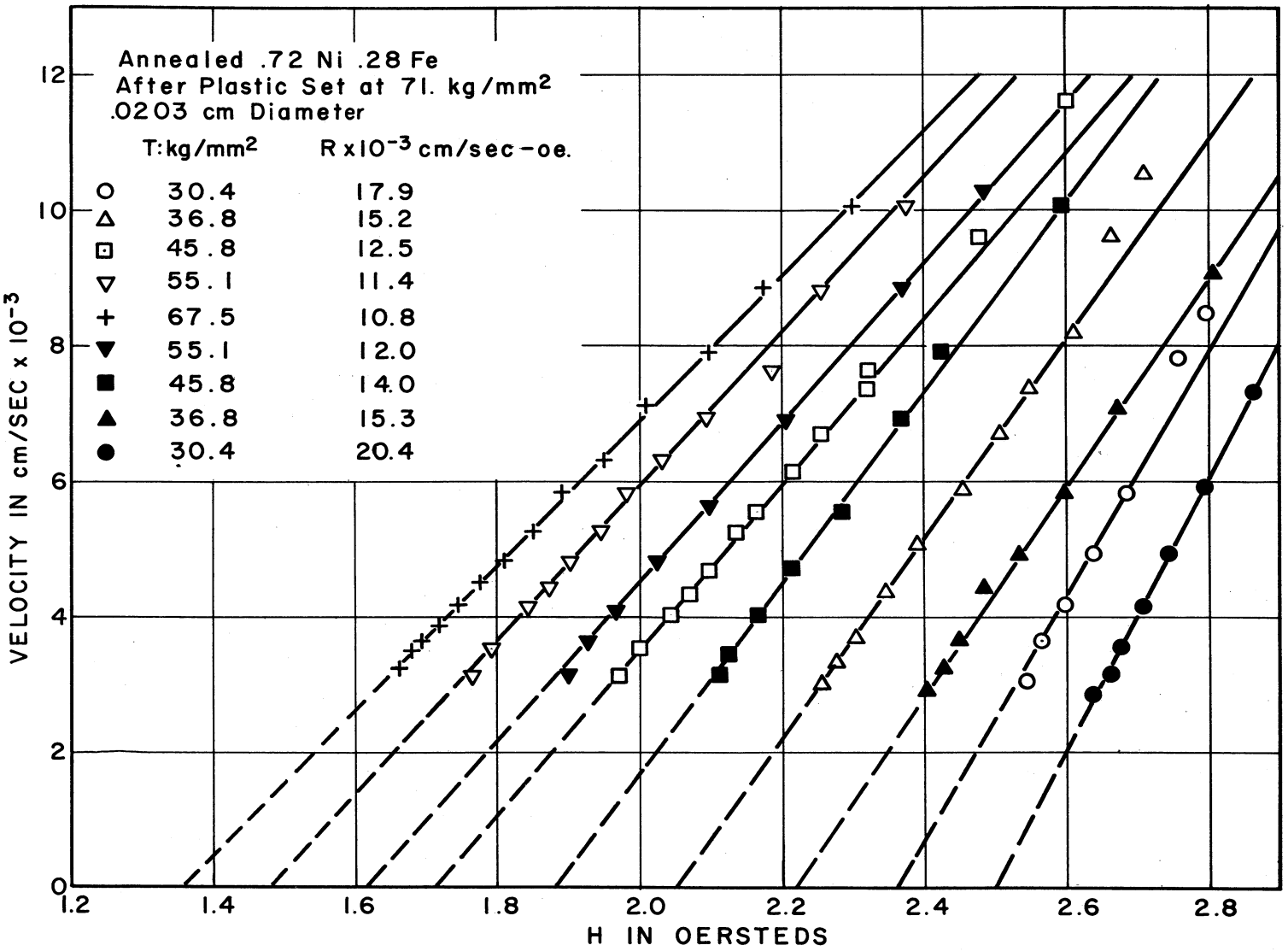

Fig. 5. Axial wall velocity vs. applied field for a .020 cm permalloy wire under tension.

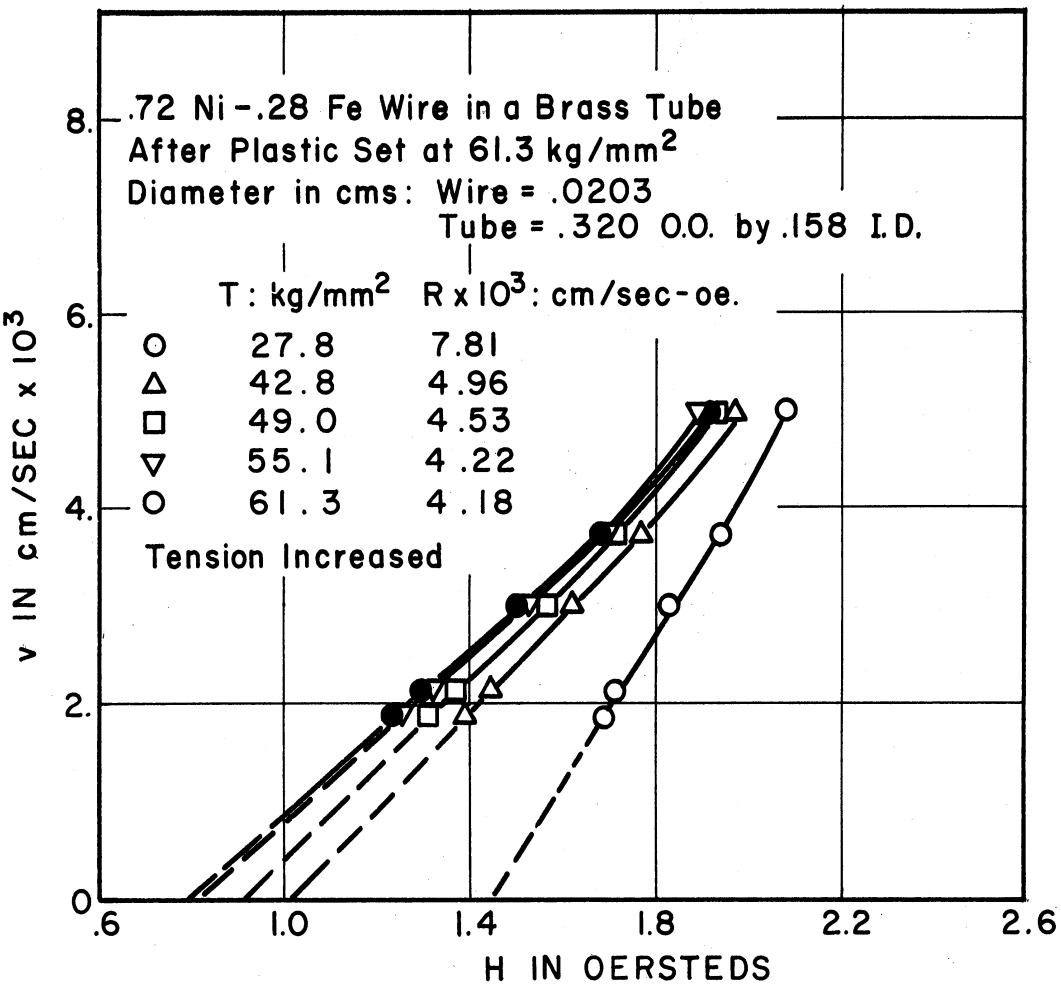

Fig. 6. Wall velocity vs. applied field for a .020 cm permalloy wire in an eddy current damping tube.

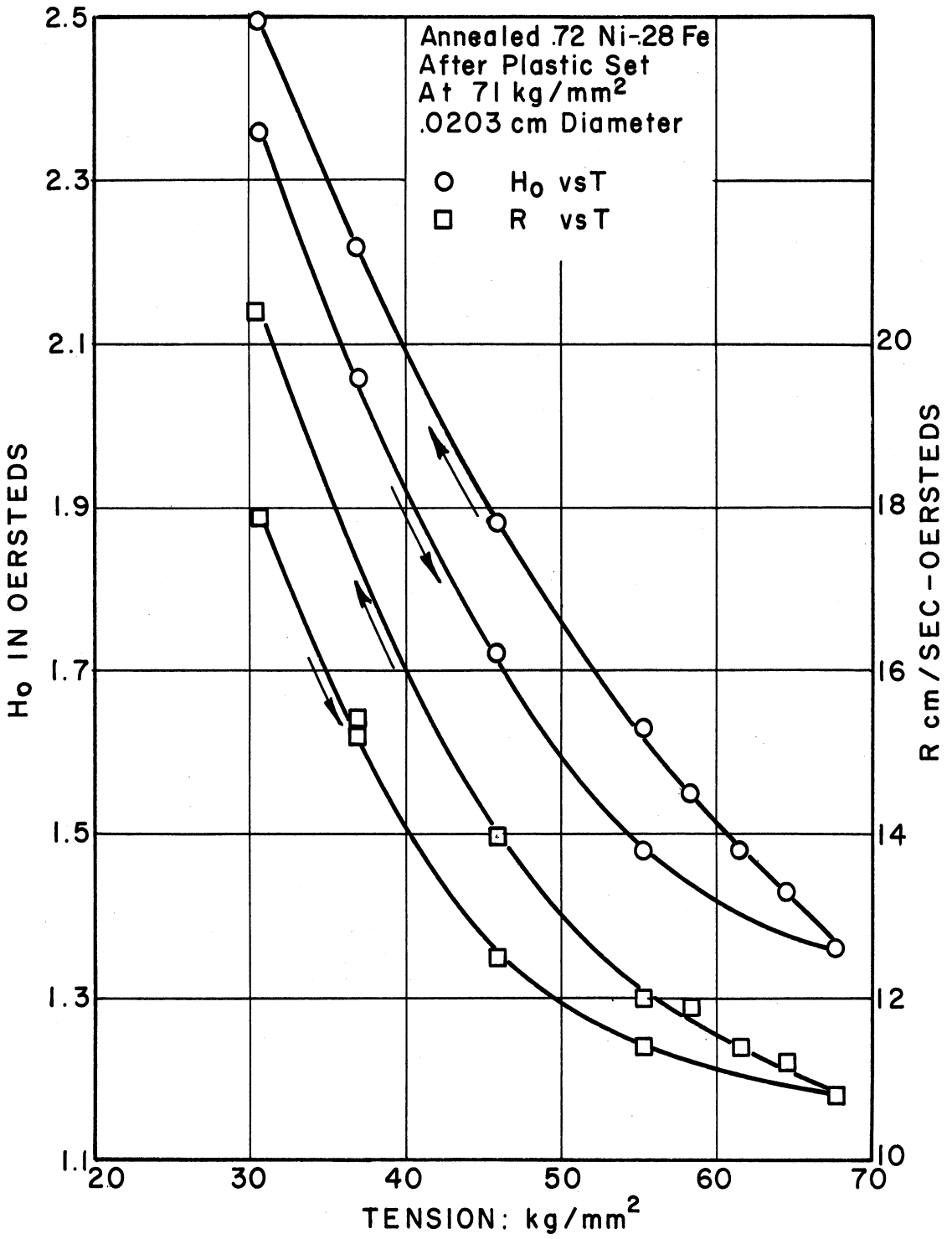

Fig. 7. Hysteresis of H_0 and R with change in tension in a .020 cm permalloy wire.

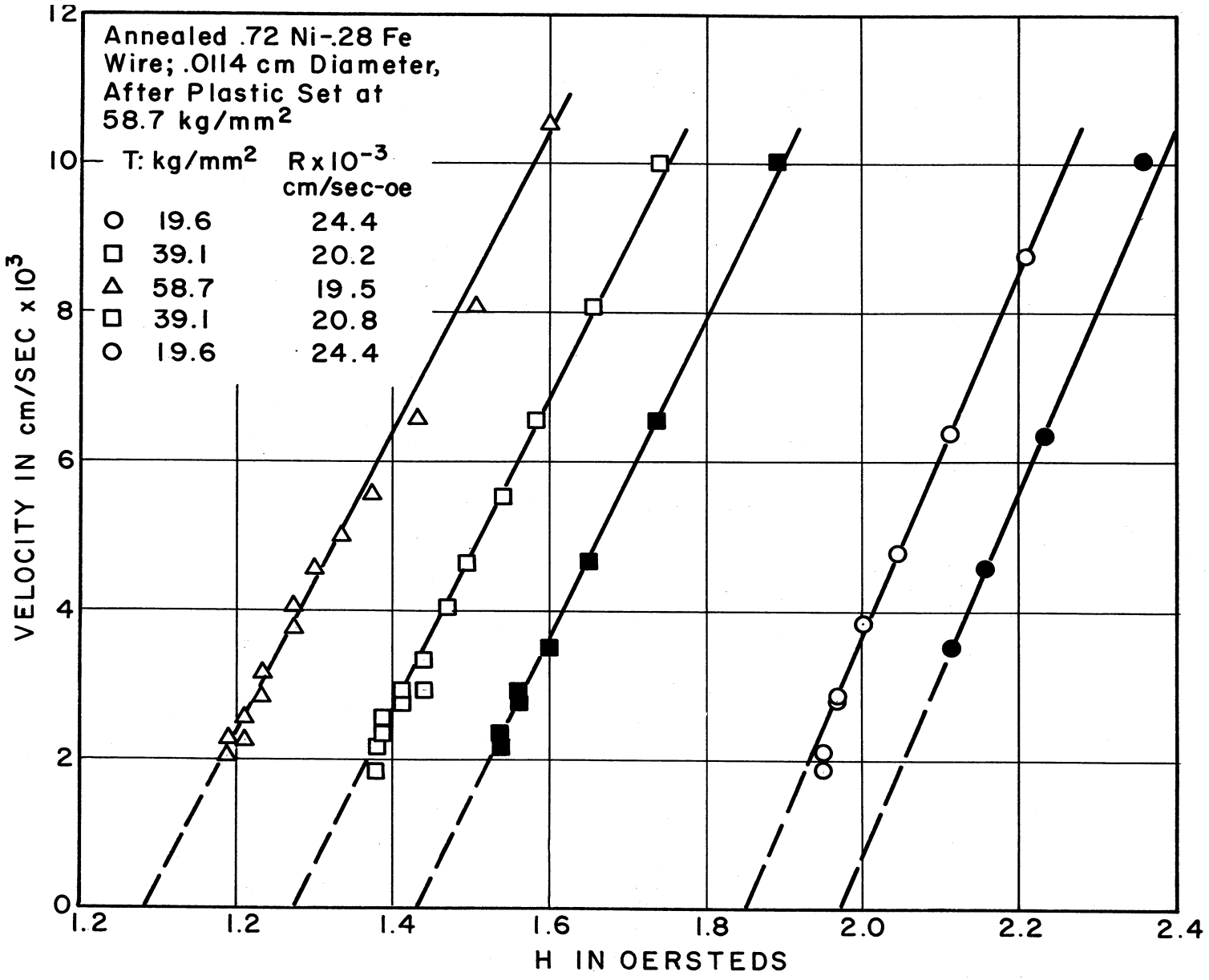

Fig. 8. Axial wall velocity vs. applied field for a .0114 cm permalloy wire under tension.

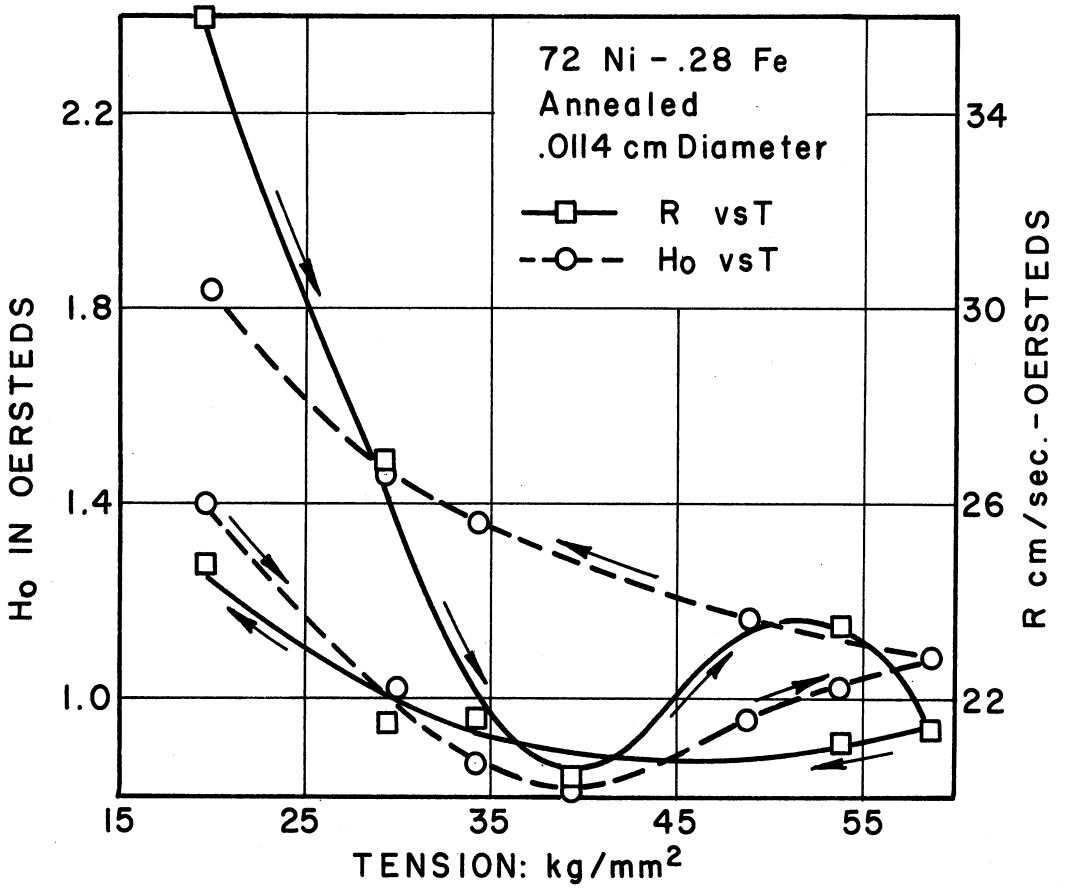

Fig. 9. Hysteresis of H_o and R with change in tension in a .0114 cm annealed permalloy wire.

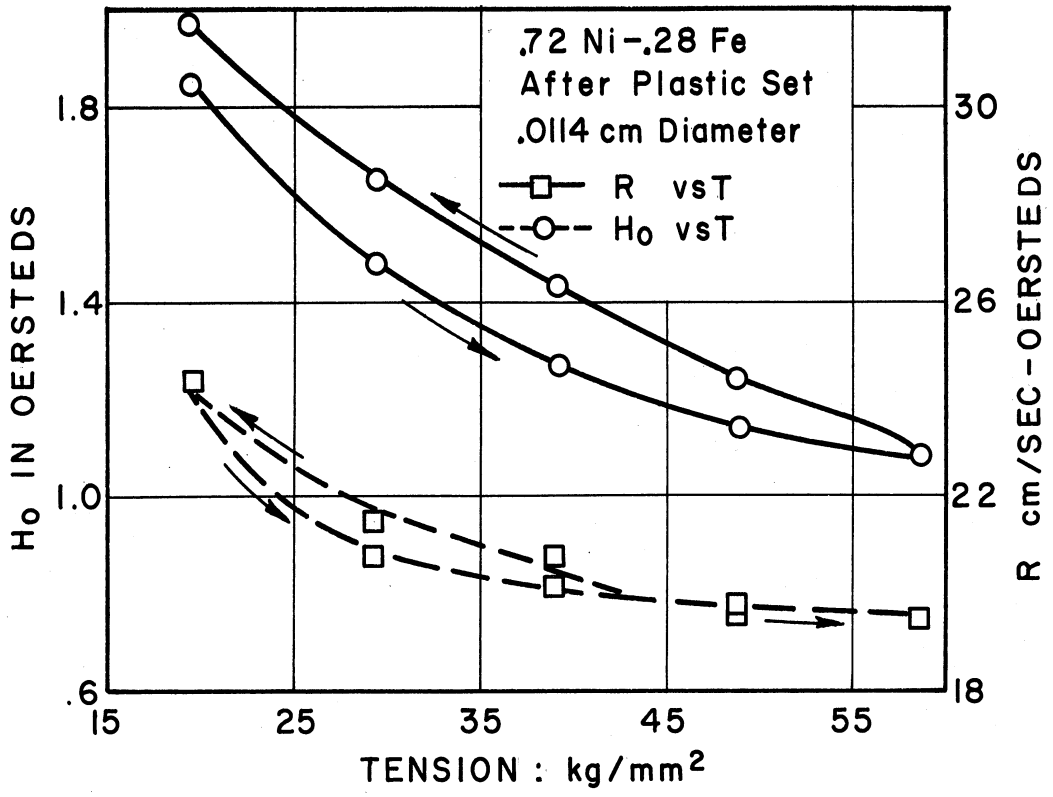

Fig. 10. Hysteresis of H_o and R with change in tension in a .0114 cm permalloy wire after plastic stretch.

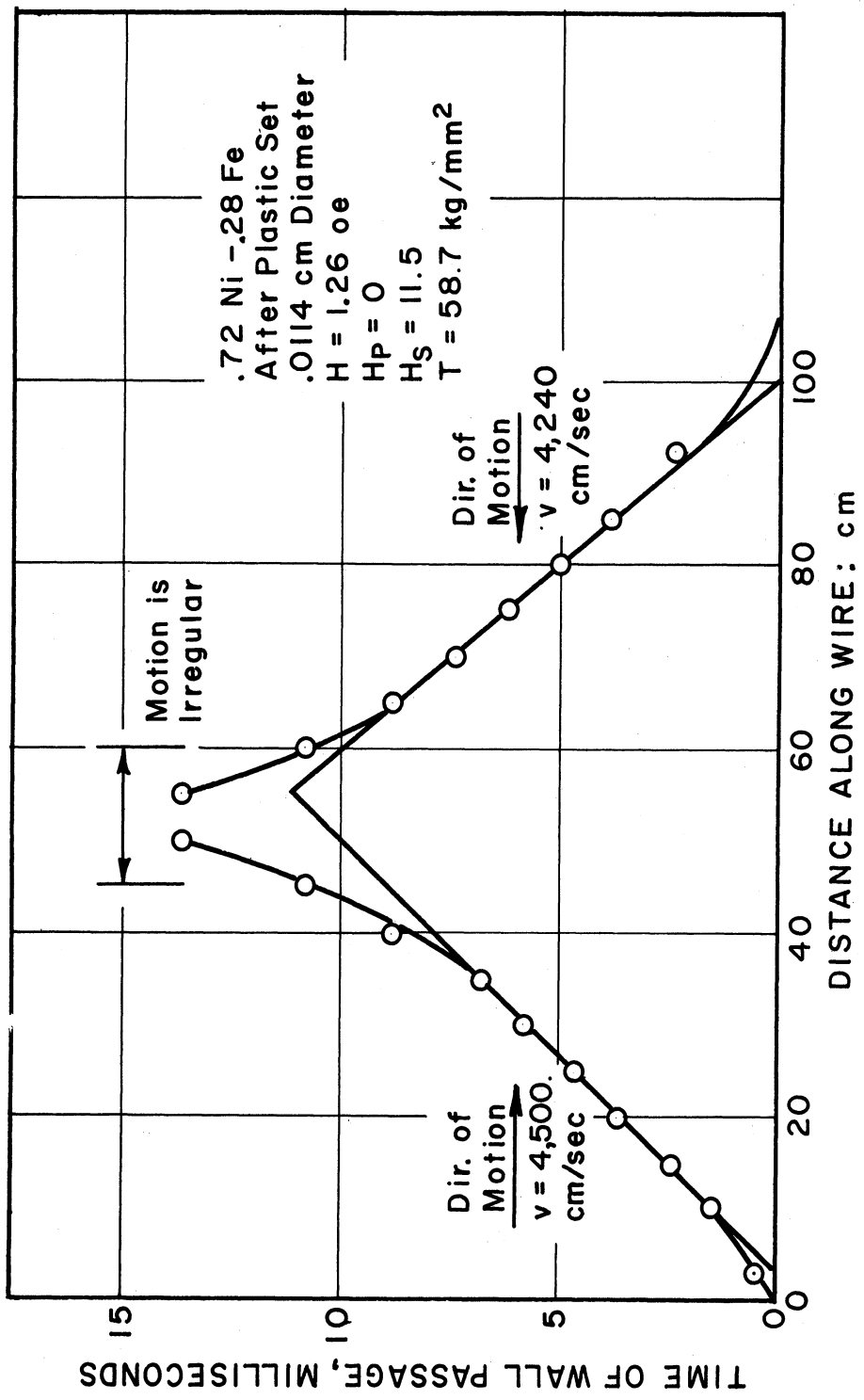

Fig. 11. Motion of domain walls nucleated at the ends of main solenoid.

REFERENCE

1. Sixtus, K. J. and Tonks, L., "Propagation of Large Barkhausen Discontinuities," Phys. Rev. 37, 930 (1931).
"Further Experiments on the Propagation of Large Barkhausen Discontinuities," Phys. Rev. 39, 357 (1932a).
"Propagation of Large Barkhausen Discontinuities II," Phys. Rev. 42, 419 (1932b).
"Propagation of Large Barkhausen Discontinuities III, Effect of Circular Field with Torsion," Phys. Rev. 43, 70 (1933a).
"Propagation of Large Barkhausen Discontinuities IV, Regions of Reversed Magnetization," Phys. Rev. 43, 931 (1933b).

2. Gyorgy, E. M., "Flux Reversal in Soft Ferromagnetics," J. Appl. Phys. 31, 110-S (1960).

3a. Kittel, C., and Galt, J. K., "Ferromagnetic Domain Theory," Solid State Physics 3, 439 (1956).

3b. Bozorth, R. M., "Ferromagnetism," D. Van Nostrand Co. (1951).

3c. Stewart, K. H., "Ferromagnetic Domains," Cambridge University Press (1954).

4. Bozorth, R. M., and Walker, J. G., "Magnetic Crystal Anisotropy and Magnetostriction in Iron-Nickel Alloys," Phys. Rev. 89, 624 (1953).

5. Ferguson, E. T., "Uniaxial Anisotropy Induced in Fe - Ni Alloys by Magnetic Anneal," J. Appl. Phys. 29, 252 (1958).

6. Gilbert, T. L., and Kelley, J. M., "Anomalous Rotational Damping in Ferromagnetic Sheets," Proc. Pitt. Conf. on Mag. and Mag. Mat., AIEE, T-78, 253 (1955).

7. Menyuk, N., "Magnetic Materials for Digital Computer Components II. Magnetic Characteristics of Ultra-Thin Mo-Permalloy Cores," J. Appl. Phys. 26, 692 (1955).

8. Haake, H., "Uber die Keime und die Ausbreitung der Ummagnetisierung bei grossen Barkhausen-Sprungen," Z. f. Phys. 113, 218 (1939).

9. Reinhart, R. E., "Large Barkhausen Discontinuities and their Propagation in Ni - Fe Alloys," Part I, Phys. Rev. 45, 420 (1934); Part II, Phys. Rev. 45, 483 (1934).

10. Dijkstra, L. J., and Snoek, J. L., "On the Propagation of Large Barkhausen Discontinuities in Ni - Fe Alloys," Philips Res. Rep. 4, 334 (1949).

11. Ogawa, S., "Uber der grossen Barkhausensprung. Dritter Teil. Anwachsen und Verschwinden des Ummagnetisierungskeimes," Sci. Rep. Tohoku Univ. 1, 53 (1949).

12. Cole, R. W., "Motion of Ferromagnetic Domain Walls in .48 Ni - Fe Tapes," J. Appl. Phys. 27, 1104 (1956).

13. Doring, W., "Uber das Anwachsen der Ummagnetisierungskeime bei grossen Barkhausen - Sprungen," Z. f. Phys. 108, 137 (1937).

14. Brown, W. F., Jr., "Micromagnetics, Domains and Resonance," J. Appl. Phys. 30, 62-S (1959).

15. Williams, H. J., and Schockley, W., and Kittel, C., "Studies of the Propagation Velocity of a Ferromagnetic Domain Boundary," Phys. Rev. 80, 1090 (1950).

16. Galt, J. K., Andrus, J., and Hopper, H. G., "Motion of Domain Walls in Ferrite Crystals," Rev. Mod. Phys. 25, 93 (1953).

17. Galt, J. K., "Motion of Individual Domain Walls in a Nickel-Iron Ferrite," Bell Sys. Tech. J. 33, 1023 (1954).

18. Galt, J. K., "Motion of a Ferromagnetic Domain Wall in Fe_3O_4," Phys. Rev. 85, 664 (1952).

19. Dillon, J. F., and Earl, H. E., "Domain Wall Motion and Ferrimagnetic Resonance in a Manganese Ferrite," J. Appl. Phys. 30, 202 (1959).

20. DeBlois, R. W., "Magnetization Processes: Reversals and Losses," J. Appl. Phys. 29, 459 (1958).

21. Olmen, R. W., and Mitchell, E. M., "Slow Domain Wall Motion in Homogeneous Vacuum Deposited Iron-Nickel Films," J. Appl. Phys. 20, 258-S (1959).

22. Neurath, P. W., "The Effect of Plastic and Elastic Stresses on the Losses and the Domain Configurations of Grain Oriented 3% Si - Fe," Proc. Pitt. Conf. on Mag. and Mag. Mat., AIEE, T-78, 92 (1955).

23. Chikazumi, S., "Magnetic Anisotropy Induced by Magnetic Annealing and by Cold Working of Ni_3Fe Crystals," J. Appl. Phys. 29, 346 (1958).

24. Rodbell D. S., and Bean, C. P., "Influence of Pulsed Magnetic Fields on the Reversal of Magnetization in Square Loop Metallic Tapes," J. Appl. Phys. 26, 1318 (1955).

25. Long, T. R., "Electrodeposited Memory Elements for a Nondestructive Memory," J. Appl. Phys. 31, 123-S (1960).

26. Broadbent, K. D., and McClung, F. J., "A Thin Magnetic Film Shift Register," Hughes Res. Lab., Res. Rept. 136 (1960).

27. Lilley, B., "Energies and Widths of Domain Boundaries in Ferromagnetics," Phil. Mag. 41, 792 (1950).

28. Becker, R., "Dynamics of the Block Wall and Permeability of High Frequencies," J. Phys. Rad. 12, 332 (1951).

29. Doring, W., "Uber die Tragheit der Wande Zwischen Weisschen Bezirken," Z. f. Natur. 3A, 373 (1948).

30. Weertman, J. R., and Rado, G. T., "Low Temperature Spin-Wave Resonance at 3,000 and 4,000 mc in a Permalloy Having Nearly Zero Magneto-crystalline Anisotropy," J. Appl. Phys. 29, 328 (1958).